Food & Function

ROYAL SOCIETY OF CHEMISTRY

PAPER

View Article Online
View Journal | View Issue

Check for updates

Cite this: *Food Funct.*, 2024, **15**, 7214

Olive oil tyrosols reduce α-synuclein aggregation *in vitro* and *in vivo* after ingestion in a *Caenorhabditis elegans* Parkinson's model†

Samanta Hernández-García, ‡ Beatriz García-Cano,‡ Pedro Martínez-Rodríguez, Paula Henarejos-Escudero and Fernando Gandía-Herrero *

Parkinson's disease is the neurodegenerative motor disorder with the highest incidence worldwide. Among other factors, Parkinson's disease is caused by the accumulation of α-synuclein aggregates in a patient's brain. In this work, five molecules present in the diet are proposed as possible nutraceuticals to prevent and/or reduce the formation of α-synuclein oligomers that lead to Parkinson's disease. The olive oil polyphenols tyrosol, hydroxytyrosol (HT), hydroxytyrosol acetate (HTA) and dihydroxyphenyl acetic acid (DOPAC) besides vitamin C were tested using a cellular model of α-synuclein aggregation and a *Caenorhabditis elegans* Parkinson's disease animal model. Levodopa was included in the assays as the main drug prescribed to treat the disease as well as dopamine, its direct metabolite. HTA and DOPAC completely hindered α-synuclein aggregation *in vitro*, while dopamine reduced the aggregation by 28.7%. The Parallel Artificial Membrane Permeability Assay (PAMPA) showed that HTA had the highest permeability through brain lipids among the compounds tested. Furthermore, the *C. elegans* Parkinson's disease model made it possible to assess the chosen compounds *in vivo*. The more effective substances *in vivo* were DOPAC and HTA which reduced the αS aggregation inside the animals by 79.2% and 76.2%, respectively. Moreover, dopamine also reduced the aggregates by 67.4% in the *in vivo* experiment. Thus, the results reveal the potential of olive oil tyrosols as nutraceuticals against α-synuclein aggregation.

Received 9th April 2024,
Accepted 14th May 2024

DOI: 10.1039/d4fo01663g

rsc.li/food-function

Open Access Article. Published on 16 May 2024. Downloaded on 1/29/2025 4:27:49 PM.
This article is licensed under a Creative Commons Attribution-NonCommercial 3.0 Unported Licence.

Introduction

Parkinson's disease (PD) is a chronic neurodegenerative disorder. Common symptoms include loss of balance, impaired postural reflexes, loss of facial expression, increased salivation, slowness of movement, and gait disorders. However, the most common and characteristic symptom is limb tremor. In fact, PD occupies the first place in the prevalence of diseases related to movement disorders, and it is the second neurodegenerative disorder, only preceded by Alzheimer's disease.[1] In addition, it is a disease associated with aging[2] that affects both sexes, with discrete predilection for males.[3]

The trigger for PD is the progressive loss of dopaminergic neurons from the substantia nigra and the simultaneous loss of dopaminergic terminals in the caudate-putamen, which is the main projection area of neurons from substantia nigra. However, the etiology of PD is still unknown, with several environmental and genetic factors that may contribute to its physiopathology.[4]

In terms of the epidemiological approach to PD, it has shown limitations since the earliest studies due to the absence of a biological marker and universally accepted diagnostic criteria. This makes the comparison between the different studies on the disease difficult.[5] Recent studies suggest that mitochondrial dysfunction and oxidative stress involving the α-synuclein (αS) protein in the neuronal cells are largely responsible for the accumulation of phosphorylated αS aggregates in the patient's brain.[6]

Currently, there is no treatment able to cure Parkinson's disease. Available treatments are only focused on the control of symptoms. Levodopa (L-dopa) remains the most prescribed drug for this disease since, unlike dopamine, it is able to cross the blood–brain barrier (BBB) and act on different metabolic pathways at the neuronal level[7]. Once crossing the blood–brain barrier, L-dopa is metabolized to dopamine by the enzyme DOPA decarboxylase, and the increase of free dopamine leads

Departamento de Bioquímica y Biología Molecular A, Unidad Docente de Biología, Facultad de Veterinaria. Regional Campus of International Excellence "Campus Mare Nostrum". Universidad de Murcia, Murcia, Spain. E-mail: fgandia@um.es; Fax: +34 868 884147; Tel: +34 868 889592

†Electronic supplementary information (ESI) available. See DOI: https://doi.org/10.1039/d4fo01663g

‡Co-first authors.

This journal is © The Royal Society of Chemistry 2024

Open Access Article. Published on 16 May 2024. Downloaded on 1/29/2025 4:27:49 PM.
This article is licensed under a Creative Commons Attribution-NonCommercial 3.0 Unported Licence.

to the recovery of synaptic transmission of dopaminergic neurons. The patient experiences a remarkable improvement in the classic symptomatology of the disease. However, after a few years, approximately 40% of patients develop secondary complications, characterized by a decrease in the drug's effectiveness, along with the emergence of spontaneous movements.[8] Therefore, it is necessary to find alternative treatments for Parkinson's disease to further control the disease evolution. In this scenario, it is of special interest to identify molecules with the potential to interfere with αS aggregation, such as polyphenols. Tyrosols are a class of polyphenols present in different quantities in olive leaves, olive fruits, and extra virgin olive oil.[9] Several studies have shown tyrosols' potent antioxidant properties, and promising results have been obtained in previous experiments on the treatment of neurodegenerative diseases.[10,11] Tyrosol is a simple phenolic compound found in a variety of plants, in addition to olives. It has been shown to possess antioxidant and anti-inflammatory properties, which may contribute to the prevention of chronic diseases such as cardiovascular disease and cancer.[12] Hydroxytyrosol (HT) is a more potent antioxidant and it is considered one of the most abundant polyphenols in olive oil. It has been shown to have a wide range of health benefits, including the prevention of cardiovascular disease, neurodegenerative diseases, and cancer.[12] Its derivative hydroxytyrosol acetate (HTA) is formed during the production of olive oil. It has been shown to have similar antioxidant and anti-inflammatory properties to hydroxytyrosol, but with higher stability and bioavailability.[13] This makes HTA a promising candidate to be used as a nutraceutical. Another polyphenol in olive oil found to possess antioxidant and anti-inflammatory properties is dihydroxyphenyl acetic acid (DOPAC). It is also a metabolite of dopamine, a neurotransmitter involved in various brain functions.[14]

On the other hand, vitamin C (sodium ascorbate) is a water-soluble antioxidant, present in citrus fruits such as oranges and grapefruits. Several studies concluded that the intake of vitamin C does not substantially affect the risk of PD in human patients;[15] however, Nagayama and coauthors reported that vitamin C improved the absorption of levodopa in elderly Parkinson's patients and concluded that a combined therapy of levodopa and ascorbic acid may ameliorate the disease symptoms.[16]

In this study, the *C. elegans* mutant strain NL5901 was used as a model of Parkinson's disease. Although *C. elegans* lacks the orthologue genes for α-synuclein (PARK1) and leucine-rich repeat kinase 2 (LRRK2), the facile manipulation of its genome allows the transgenic expression of human genes and the study of neuronal degeneration.[17] The available mutant strains WLZ1 and WLZ3 that overexpress human LRRK2 are used as a nematode model for Parkinson's disease.[18] Meanwhile, *C. elegans* strains that express human αS under the control of specific promoters allow the visualization, localization, and quantification of αS aggregates *in vivo*.[19] For example, strain NL5901 expresses αS fused with YFP in an animal's muscles, while strain ERS100 overexpresses α-synuclein fused with Venus in dopaminergic neurons marked with mCherry. Furthermore, Parkinson's neurodegeneration can be simulated by exposing nematodes to neurotoxins. Exposure to rotenone, a plant neurotoxin, or 6-OHDA (6-hydroxydopamine), a precursor of 1-methyl-4-phenylpyridinium (MPP), induces programmed cell death in dopaminergic neurons in the nematode.[20] Thus, the simple genetic manipulation and different mutant strains of *C. elegans* available offer multiple possibilities for the discovery of new targets and treatments for Parkinson's disease.

The lack of treatments aimed to reduce αS aggregation encouraged this study to assess the potential of various molecules present in the diet as possible nutraceuticals to prevent or reduce the formation of αS oligomers that cause Parkinson's disease. Olive oil polyphenols (tyrosols), dopamine, levodopa and vitamin C (Fig. 1) were evaluated as αS anti-aggregation agents using a cellular model of αS aggregation based on bimolecular fluorescence complementation (BiFC) technology and *C. elegans* mutant strain NL5901 as an animal model of Parkinson's disease.

The hypothesis of this study is that naturally occurring polyphenols, such as olive oil tyrosols, could reduce αS aggregation due to their structure, chemical characteristics, and antioxidant properties.

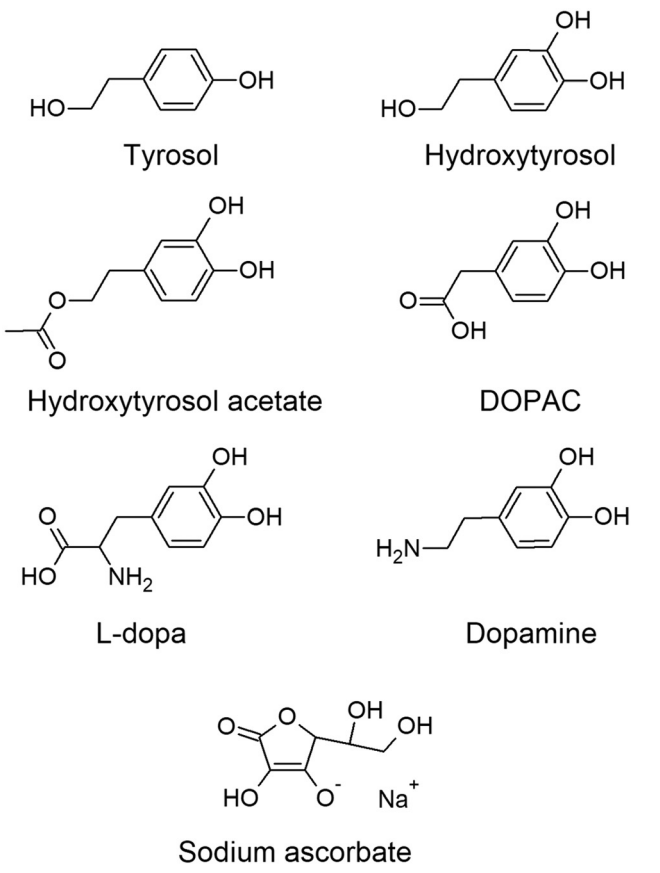

Fig. 1 Structures of the molecules used in the study.

Open Access Article. Published on 16 May 2024. Downloaded on 1/29/2025 4:27:49 PM. This article is licensed under a Creative Commons Attribution-NonCommercial 3.0 Unported Licence.

Experimental

Materials

Hydroxytyrosol (2-(3,4-dihydroxyphenyl)ethanol) and hydroxytyrosol acetate (2-(3,4-dihydroxyphenyl)ethyl acetate) were kindly donated by Seprox Biotech SL. (Murcia, Spain). Tyrosol (2-(4-hydroxyphenyl)ethanol), DOPAC (3,4-dihydroxyphenylacetic acid), dopamine (4-(2-aminoethyl)benzene-1,2-diol), L-dopa (L-3,4 dihydroxyphenylalanine) and sodium ascorbate (2,3-didehydro-L-*threo*-hexono-1,4-lactone sodium enolate) were purchased from Merck (KGaA, Darmstadt, Germany). Stock solutions were prepared in HPLC-grade water at concentrations of 7.6 mM for L-dopa, 1 mM and 15 mM for sodium ascorbate, and 100 mM for the other compounds. The stock solutions were maintained at −20 °C until use. HPLC-grade water (Fisher Scientific, United Kingdom) was used for all the experiments.

Screening of α-synuclein anti-aggregation agents

The measurement of αS aggregation *in vitro* was performed using a cellular model based on *bimolecular fluorescence complementation* (BiFC) technology developed by Eastwood and coauthors[21] (Fig. 3A). Plasmids pET-alpha-synuclein-BiFC (plasmid Addgene #87855; **https://n2t.net/addgene:87855**; RRID: Addgene_87855) and pNatB (pACYCduet-naa20-naa25) (plasmid Addgene #53613; **https://n2t.net/addgene:53613**; RRID: Addgene_53613) were kindly supplied by Dan Mulvihill. The plasmids were inserted and amplified in DH5-α competent cells. The thermocompetent strain BL21 of *E. coli* (Invitrogen, Thermo Fisher Inc., Carlsbad, California, United States) was used to perform the combined transfection of plasmids by heat shock transformation.

The BiFC cellular model was used following the authors' published protocol. Briefly, cells were cultured in LB broth until an optical density (OD_{600}) of 0.2–0.3 was reached and then diluted to 0.03 with fresh LB supplemented with ampicillin (100 μg mL^{-1}), chloramphenicol (25 μg mL^{-1}), and 1 mM isopropyl-β-D-1-thiogalactopyranoside (IPTG) as an inducer. The assays were performed in black 96-well plates and monitored using a Synergy HT microplate reader from BIO-TEK (Winooski, VT, USA). One hundred microliters of the diluted cell mixture were placed in each well, followed by the selected compound, and completed with fresh LB up to 300 μL. For each concentration, 5 replicates were made, and cell-free controls and compound-free controls were also performed. Measurements were set every 15 minutes in fluorescence mode (λ_{ex} 485 nm and λ_{em} 530 nm) with the temperature fixed at 37 °C.

2.3 Cell fluorescence microscopy

The visual verification of the aggregation assays was performed by fluorescence microscopy. Cells from cultures induced at 37 °C and treated with different molecules for 12–15 h were used. Cells were fixed on agarose pads to facilitate visualization. The pads were prepared by placing a drop of melted agarose solution (1%) on a microscope slide and pressing gently with another slide until it solidified. The cells (10 μL) were pipetted on the pads and left to air-dry until the liquid was fully absorbed, and then a cover slide was placed on top. The cells were visualized under fluorescence, using the I3 filtercube for GFP of a Leica DM 2500 LED fluorescence microscope equipped with a Leica DFC550 camera (Leica Microsystems, Wetzlar, Germany). The oil immersion technique was used to observe the samples, which allowed 100× magnification.

The fluorescence intensity of the cells was determined with ImageJ (NIH) software.[22] Briefly, each fluorescence image was divided into red, blue, and green channels, from which green was selected. Then, the threshold tool was applied so that the program could define the fluorescent zones and measure the intensity.

2.4 Parallel artificial membrane permeability assay (PAMPA)

Porcine brain lipid (PBL) was purchased from Avanti Polar Lipids (Alabaster, AL, USA). The 96-well donor microplate (PVDF membrane, pore size 0.45 μm) and the acceptor microplate were both from Merck Millipore Bioscience (Bedford, MA, USA). PAMPA was performed following the published protocol of Studzińska-Sroka and coauthors (2021),[23] with some modifications. Stock solutions of the tested compounds were prepared at 15 mM except L-dopa, which was prepared at 7.6 mM in PBS, pH 7.4. Permeability controls, verapamil and theophylline, were prepared at 4.3 mM in PBS.

The donor plates were filled with 300 μL of each compound. Then, the filter membrane of the acceptor microplate was coated with 4 μL of the PBL solution, prepared at 20 mg mL^{-1} in dodecane, and 200 μL of PBS were placed in the acceptor wells. Thereafter, the acceptor plate was gently placed into the donor plate and incubated at 37 °C for 4 hours in a humidity chamber. At the end of the assay, the molecules were detected in the acceptor and donor plates by HPLC using a C18 column. Compound permeability was calculated with the following equation (eqn (1))

$$P_e = -\frac{\ln\left(1 - \frac{C_A}{C_{eq}}\right)}{S \times \left(\frac{1}{V_D} + \frac{1}{V_A}\right) \times t} \quad (1)$$

where P_e is the effective permeability coefficient (cm s^{-1}), V_D and V_A are volumes in donor and acceptor wells (cm^3), C_A is the concentration in the acceptor plate, S is the membrane area (0.28 cm^2), t is the experiment time in seconds, and C_{eq} is the concentration in the equilibrium calculated with eqn (2).

$$C_{eq} = \frac{(V_D \times C_D) + (V_A \times C_A)}{V_D + V_A} \quad (2)$$

Verapamil is a control classified as a high-permeability drug and theophylline is a low-permeability drug.

Caenorhabditis elegans strain and maintenance

The strain of *C. elegans* NL5901 *pkIs2386 [unc-54p::alphasynuclein::YFP + unc-119(+)]* was kindly donated by the Caenorhabditis Genetic Center (CGC, Saint Paul, Minnesota,

 This journal is © The Royal Society of Chemistry 2024

Open Access Article. Published on 16 May 2024. Downloaded on 1/29/2025 4:27:49 PM.
This article is licensed under a Creative Commons Attribution-NonCommercial 3.0 Unported Licence.

United States), which is funded by the "NIH Office of Research Infrastructure Programs" (P40 OD010440). This strain was maintained following the protocols established by Stiernagle.[24] All experiments were performed with synchronous cohorts of *C. elegans* prepared using the bleach method.

Measurement of α-synuclein aggregation on the *C. elegans* model of Parkinson's disease

The strain NL5901 was used to study the effect of the different compounds by measuring their potential to reduce the formation of αS aggregates *in vivo*. The nematodes in the L1 stage were transferred to 5 mL flasks containing S medium, supplemented with 500 µL of concentrated 10× *E. coli* OP50 and the selected compounds. The molecules were tested at 15 mM in combination with 1 mM sodium ascorbate; additionally, a control without compounds and a control with 1 mM sodium ascorbate were performed. On the second day of development, when animals are between the L4 and young adult stages, 100 µL of FUdR (2′-deoxy-5-fluorouridine) prepared at 10 mg mL^{-1} was added to the flask to avoid the progeny during the assays.[25] The animals were visualized for several days to study the αS aggregation progress over time; thus, samples were taken at the 1st, 4th, and 7th days of development. The nematodes were washed with M9 buffer and mounted on microscope slides that already contained sodium azide (10 mM) as an anesthetic. The images were taken with the Leica DM 2500 LED fluorescence microscope at 40× magnification. ImageJ was used to measure the fluorescence of the head–pharynx area of each nematode.

Lifespan assays

C. elegans lifespan was measured automatically using the lifespan machine following the published protocols of Guerrero-Rubio and coauthors.[26] The nematodes of the strain NL5901 were treated with the bioactive compounds for 48 hours at 20 °C before transferring them to the NGM-agar analysis plates supplemented with FdUR at 10 µg mL^{-1} to control the progeny.

Statistical analysis

Survival data obtained from the lifespan machine were analyzed using the Sigmaplot 14.0 software (Systat Software Inc., Palo Alto, California, United States) with the Kaplan–Meier estimator and the *F*-test. The statistics of the rest of the assays were obtained with the Sigmaplot software using the ANOVA statistical test with a confidence interval of 95%.

Results and discussion

Effect of polyphenols on α-synuclein aggregation in the bimolecular fluorescence cellular model

The αS-BiFC cell model[21] was used to evaluate the formation kinetics of αS oligomers in the presence and absence of potential antiaggregating molecules. Monitoring the increase of fluorescence over time, kinetic curves are obtained (Fig. 2A), in which fluorescence increases rapidly to reach a plateau thereafter. To obtain the aggregation rate, the highest slope for each condition is determined between the first 10 and 300 minutes.

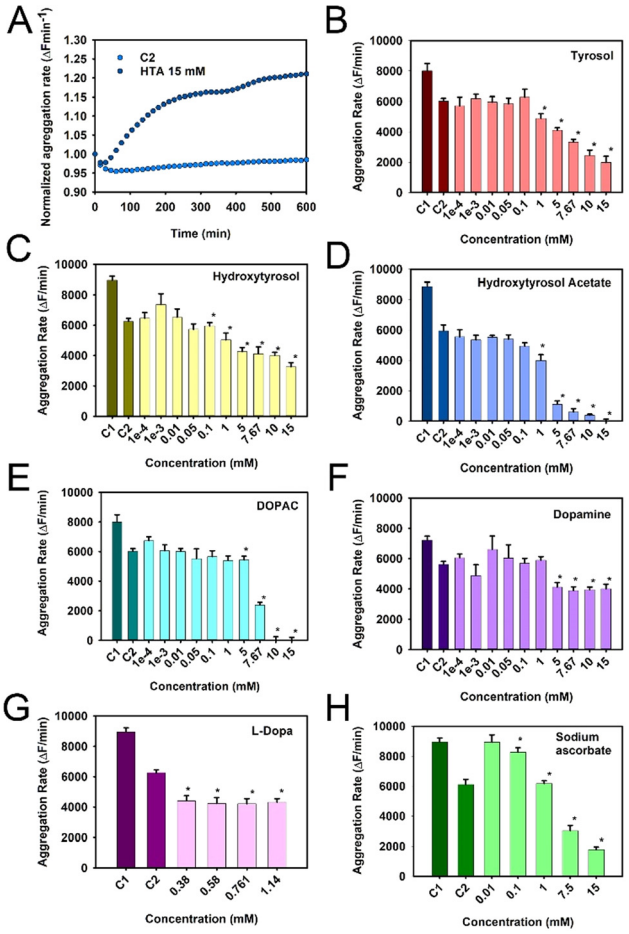

Fig. 2 Effect of bioactive molecules stabilized with 1 mM sodium ascorbate on the αS aggregation rate. (A) Representative aggregation curves for the control condition and the treatment with hydroxytyrosol acetate at 15 mM. (B–E) Compounds' dose-dependence assays. (B) Tyrosol stabilized with sodium ascorbate (1 mM). (C) Hydroxytyrosol acetate stabilized with sodium ascorbate. (D) Hydroxytyrosol stabilized with sodium ascorbate. (E) DOPAC stabilized with sodium ascorbate. (F) Dopamine stabilized with sodium ascorbate. (G) L-Dopa stabilized with sodium ascorbate. (H) Sodium ascorbate. Data are represented as mean ± standard deviation of 5 replicates per condition, * *p*-value ≤0.05 by ANOVA test using Bonferroni *post hoc* test. C1 is the control and C2 is the control supplemented with 1 mM sodium ascorbate.

Screening experiments were performed with natural molecules of high biological interest to find compounds able to delay and/or decrease the αS aggregation in the BiFC model. The compounds chosen were tyrosol, hydroxytyrosol, hydroxytyrosol acetate, DOPAC and dopamine. These molecules at low concentrations were mildly effective (Fig. S1 and Table S1†) due to the molecules' oxidation, as evidenced by a dark coloration in the test flasks at the end of the experiments (Fig. S1F†), and by the exponential increase in fluorescence not related to αS aggregation. Therefore, the concentration of

Open Access Article. Published on 16 May 2024. Downloaded on 1/29/2025 4:27:49 PM.
This article is licensed under a Creative Commons Attribution-NonCommercial 3.0 Unported Licence.

the molecules was increased and L-dopa and vitamin C (sodium ascorbate) were added to the screening assays. Sodium ascorbate at 1 mM was used to supplement each test compound as an antioxidant in order to avoid the autoxidation of the molecules and the formation of *o*-quinones.[27] Once the complementary treatment with sodium ascorbate was established, measurements of the interference of the αS aggregation were performed using tyrosol, hydroxytyrosol, hydroxytyrosol acetate, DOPAC, and dopamine in a range of concentrations from 0.0001 to 15 mM (Fig. 2B–F). The concentration range for L-dopa was lower (Fig. 2G) due to its low solubility in water (1.14 to 0.38 mM). Additionally, sodium ascorbate was also tested in a concentration range from 0.01 to 15 mM (Fig. 2H). Overall, the tested compound reduced the oligomerization rate of αS in comparison with the controls in the cell model, suggesting the effectiveness of these molecules as αS anti-aggregation agents. Although most compounds at concentrations below 1 mM did not reduce the aggregation rate, hydroxytyrosol acetate (Fig. 2C) and sodium ascorbate (Fig. 2H) significantly reduced the rate of oligomer aggregation by 16.9% and 7.7%, respectively, at a concentration of 0.1 mM. Furthermore, L-dopa was able to reduce the rate of αS oligomerization by 12.0% at 0.38 mM (Fig. 2G).

The reduction percentages given in ESI Table S1† were calculated with respect to the control without ascorbate, while in ESI Table S2,† they are referred to the control with 1 mM sodium ascorbate. Therefore, in some cases, the percentage of reduction shown in ESI Table S1 is higher than that in ESI Table S2.† In comparison with the ascorbate-free control, hydroxytyrosol acetate reduced the aggregation rate by 55.0%. It is noteworthy that the effects of sodium ascorbate combined with hydroxytyrosol acetate were not additive but synergistic, *i.e.*, the effect on the αS aggregation rate using the combination of both substances is higher than that with the addition of the individual substances.

The treatment with 10 and 15 mM DOPAC totally hindered the αS aggregation (Fig. 2E, ESI Table S2†), while hydroxytyrosol acetate and sodium ascorbate at 15 mM decreased the rate of aggregate formation by 99.6 and 80.2%, respectively (Fig. 2C and H). Furthermore, tyrosol and hydroxytyrosol reduced the aggregation rate by 67.0 and 47.0%, respectively (Fig. 2B and C). Dopamine had a lower effect (Fig. 2F) compared to the other compounds tested (28.7%), and the effect was not dose-dependent. The results showed that the effective concentrations *in vitro* are high, and thus it could be difficult to achieve these concentrations by only consuming hydroxytyrosol-containing foods. Extra virgin olive oil (EVOO) has an average hydroxytyrosol concentration of 14.32 mg kg^{-1}, while olives like Spanish green olives and Greek kalamata olives have a concentration of 170–510 mg kg^{-1} and 250–760 mg kg^{-1}, respectively.[28] As a result, following a Mediterranean diet, the consumption of this molecule could be up to 5 mg per day, although in some clinical trials, the dose has been increased to 15–25 mg per day. Furthermore, the EFSA considered 50 mg kg^{-1} as a safe daily intake of hydroxytyrosol in adults,[29] so efforts have been made to increase the consumption of this beneficial ingredient. Supplements rich in this compound are already available for the consumer. Furthermore, it has been added to processed foods as a preserving agent and the EFSA authorized hydroxytyrosol addition to fish and vegetable oils (215 mg kg^{-1}) and spreadable fats (175 mg kg^{-1}).[29] The incorporation of hydroxytyrosol into food products increases their health-promoting benefits and lengthens their shelf life because of the antibacterial and antioxidant properties of the molecule. Moreover, several studies with mice showed that hydroxytyrosol was non-toxic up to 500 mg per kg per day (ref. 30) and Pérez de la Lastra and coauthors[31] proposed a dose of 800 mg per day for adult humans to treat SARS-CoV-2. Thus, it could be healthy to increase hydroxytyrosol consumption in the diet.

The parameter EC_{50} is a value widely used in pharmacology to estimate the efficacy of a drug. It can be defined as the required concentration of a molecule to obtain 50% of the desired effect. The more effective a compound is, the lower the IC_{50} will be. The results on the aggregation rate were adjusted to the Hill equation (eqn (1)) to obtain the EC_{50} of the molecules.

$$E = \frac{E_{\max}}{1 + \left(\frac{EC_{50}}{C}\right)^{nH}} \quad (3)$$

The compounds with lower EC_{50} values were hydroxytyrosol acetate (1.97 mM) and sodium ascorbate (2.8 mM), while DOPAC, hydroxytyrosol, and tyrosol had values of 7.5, 7.6, and 22.9 mM, respectively (ESI Fig. S2 and Table S3†). Numerous studies have described small molecules capable of inhibiting αS aggregation using different experimental methods. In 2006, Masuda and co-authors investigated the effects of 79 compounds on αS oligomerization *in vitro*, obtaining IC_{50} values in the micromolar range for some compounds such as baicalein (flavone, 8.2 μM), delfinidine (anthocyanidine, 6.5 μM), or vitamin E (α-tocopherol, 10.9 μM).[32] Further studies have shown that tolcapone and entacapone are potential inhibitors of αS, used at micromolar concentrations. These molecules belong to the class of multifunctional drugs used as adjuvants for L-dopa, as they can inhibit COMT (catechol-*O*-methyltransferase), act as antioxidants, and inhibit protein aggregation.[33]

The results obtained by the BiFC technique used to assess αS aggregation in the presence of bioactive molecules were visually verified by fluorescence microscopy (Fig. 3B–H). Cells without IPTG as an inducer did not show any fluorescence (Fig. 3B); in contrast, the control cells induced with IPTG showed the highest fluorescence (Fig. 3C). Both results are consistent with the aggregation curves obtained and the BiFC technical foundations. Compared to the control cells, all compounds decreased the fluorescence and therefore the αS oligomerization. The most relevant compounds were hydroxytyrosol acetate and DOPAC, assayed at a concentration of 15 mM and stabilized with sodium ascorbate at 1 mM. This caused the complete disappearance of fluorescence (Fig. 3G and H). At the same concentration, sodium ascorbate managed to decrease the fluorescence by 78.8% (Fig. 3E). In addition, a low dose (1 mM) of vitamin C and hydroxytyrosol reduced the

 This journal is © The Royal Society of Chemistry 2024

Open Access Article. Published on 16 May 2024. Downloaded on 1/29/2025 4:27:49 PM.
This article is licensed under a Creative Commons Attribution-NonCommercial 3.0 Unported Licence.

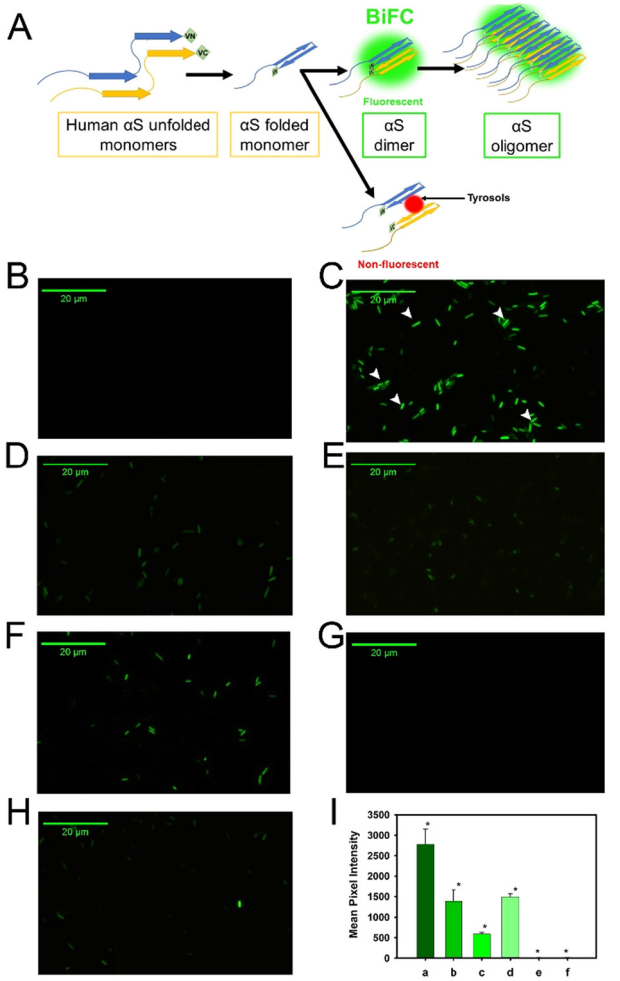

Fig. 3 Microscopy of the BiFC αS aggregation model. (A) Bimolecular fluorescence complementation technology scheme used to measure αS aggregation *in vitro*. Vn is the Venus N-terminal and Vc is the Venus C-terminal. (B–H) Representative fluorescence images of the *E. coli* cells; raw images are shown in Fig. S4.† (B) Negative control (without an inducer). (C) Positive control (cells induced with IPTG). The arrowheads point to the fluorescent cells. (D) Treatment with sodium ascorbate (1 mM). (E) Treatment with sodium ascorbate (15 mM). (F) DOPAC, 1 mM, stabilized with 1 mM sodium ascorbate. (G) DOPAC, 15 mM, stabilized with 1 mM sodium ascorbate. (H) Treatment with HTA (15 mM) stabilized with sodium ascorbate (1 mM). Scale bar: 20 μm. (I) Measurements of cell fluorescence intensity. (a) Control cells induced with IPTG. (b) Treatment with sodium ascorbate at 1 mM. (c) Treatment with sodium ascorbate at 15 mM. (d) Treatment with 1 mM DOPAC and 1 mM sodium ascorbate. (e) Treatment with DOPAC (15 mM) and sodium ascorbate (1 mM). (f) Treatment with HTA (15 mM) and sodium ascorbate (1 mM). Data are presented as mean ± standard deviation. *p-Value ≤ 0.05 by ANOVA test using Bonferroni *post hoc* test.

fluorescence intensity of the cells by 46.3% and 50.0%, respectively.

Effective permeability of tyrosols

The parallel artificial membrane permeability assay (PAMPA) was performed to evaluate *in vitro* the permeation of the molecules through the blood–brain barrier (BBB) (Fig. 4). The

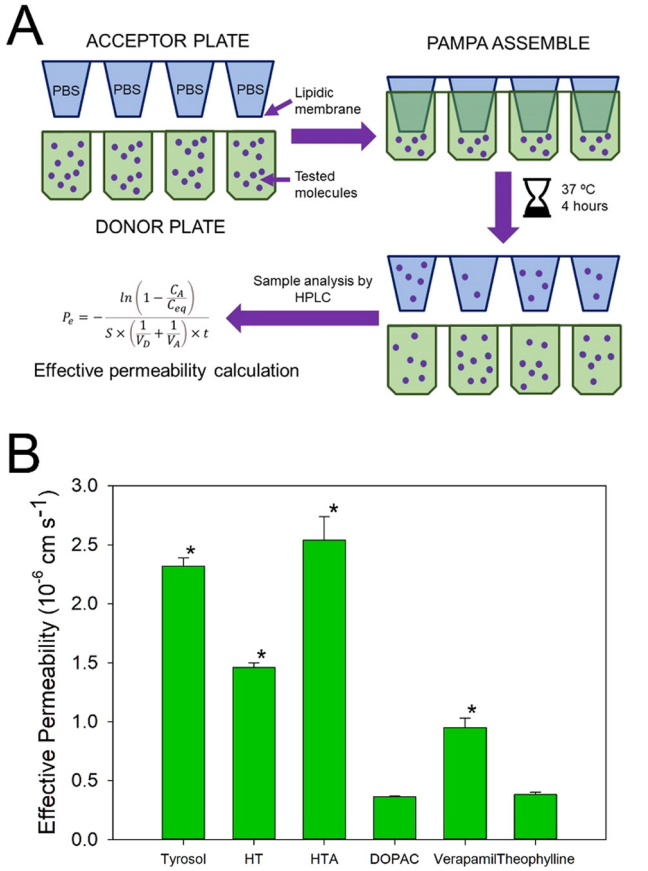

Fig. 4 Parallel artificial membrane permeability assay. (A) Experiment overview. (B) Effective permeability data are presented as mean ± standard deviation* p-value *vs.* theophylline ≤0.05 by T-test. The compounds were assayed in triplicate, and two independent experiments were performed.

obtained effective permeability (P_e) for verapamil, a highly permeable molecule, was 0.95 ± 0.08 (10^{-6} cm s^{-1}), whereas for the low permeability molecule, theophylline, P_e was 0.38 ± 0.02 (10^{-6} cm s^{-1}). The compounds dopamine, L-dopa and ascorbate were not detected in the acceptor wells, thus showing low permeability under the experimental conditions. Hydroxytyrosol acetate had a higher P_e with a value of 2.54 ± 0.2 (10^{-6} cm s^{-1}), 2-fold higher than that of verapamil, while DOPAC had a value of 0.36 ± 0.01 (10^{-6} cm s^{-1}). This may indicate that the presence of a carboxylic group reduced the capacity of the molecule to cross the membrane. Moreover, the presence of additional hydroxyl groups also hampered the effective permeability, as shown by the values for tyrosol and hydroxytyrosol: 2.32 ± 0.07 and 1.46 ± 0.04 (10^{-6} cm s^{-1}), respectively. Interestingly, HTA is the ester derivative of hydroxytyrosol, and thus it has the same structure except for the acetic acid linked by an ester bond to the phenol moiety. The esterification of the hydroxyl groups could be a way to increase the membrane permeability of a chosen molecule. Overall, all the tyrosols showed better performance in the PAMPA assay than the molecule L-dopa, prescribed as a Parkinson's disease treatment.

Open Access Article. Published on 16 May 2024. Downloaded on 1/29/2025 4:27:49 PM.
This article is licensed under a Creative Commons Attribution-NonCommercial 3.0 Unported Licence.

Molecule effect on α-synuclein oligomerization *in vivo*

The visualization and quantification of αS aggregation *in vivo* were performed with a *C. elegans* NL5901 mutant strain (*pkIs2386 [unc-54p::alphasynuclein::YFP + unc-119(+)]*). The strain incorporates the transgene pkIs2386, which is a construct encoding human αS and a fluorescent yellow protein (YFP). The fused unc-54 promoter directs the expression of the transgene to muscle cells. This model allows the visual detection of αS aggregates in the muscle wall of the nematode through a fluorescence microscope.[34]

It is expected that αS-YFP fusion inclusions, which appear to be unevenly distributed fluorescent dots in *C. elegans* (Fig. 5), could represent the primary cytotoxic αS species present in the post-mortem brain tissue of human patients affected by the disease.[35]

In the nematodes, the αS protein expression and aggregation develop with aging, and show a maximum at the 4th day of adulthood (Fig. 5C1, and Fig. 6).

After 48 hours of treatment, all the bioactive molecules, except L-dopa, were able to hinder the aggregation of αS in the nematodes. Dopamine and DOPAC were the molecules that most decreased the αS aggregates *in vivo* on the first day of adulthood – by 70.8% and 74.8%, respectively (Fig. 5 and 6). However, the most stable were hydroxytyrosol acetate and DOPAC, since the antiaggregating effect was maintained over time. By the seventh day of adulthood, these molecules reduced the αS aggregates *in vivo* by 71.8% and 71.0%, respectively. Furthermore, the number of aggregates formed was also measured (Fig. S5B†), and the results obtained were similar to those obtained by the quantification of the fluorescence. DOPAC and hydroxytyrosol acetate reduced the number of aggregates by 68.6% and 58.1%, respectively, on the 4th day of adulthood. Interestingly, L-dopa did not significantly reduce the formation of aggregates on *C. elegans*, while dopamine, the decarboxylated metabolite of L-dopa, and the active principle within the blood–brain barrier, was effective in hindering the αS aggregation. Dopamine may be more effective than L-dopa on *C. elegans*, probably because the nematode lacks a blood–brain barrier, although the glial cells that cover the cephalic sensory neurons may act as a simple blood–brain barrier.[36] Other studies have tested the effect of small molecules on αS aggregation. Saewanee and coauthors used the antidiabetic drug metformin on the *C. elegans* NL5901 strain, and the results showed that metformin at 15 mM reduced the αS aggregation *in vivo* by 19.6% on the fourth day of adulthood.[37] Hughes and coauthors tested levodopa (L-dopa) at 1 mM on the same *C. elegans* strain, and the results obtained indicated that L-dopa at 1 mM did not have an effect on αS aggregation; however, at 3 mM the aggerates were reduced by 30%. The authors also tested other molecules and concluded that valproic acid, bexarotene, galantamine, and tetrabenazine reduced the synuclein plaques when used in a concentration range of 1 to 3 mM.[38]

The inhibitory effects of hydroxytyrosol acetate and DOPAC on αS aggregation can be attributed to various underlying

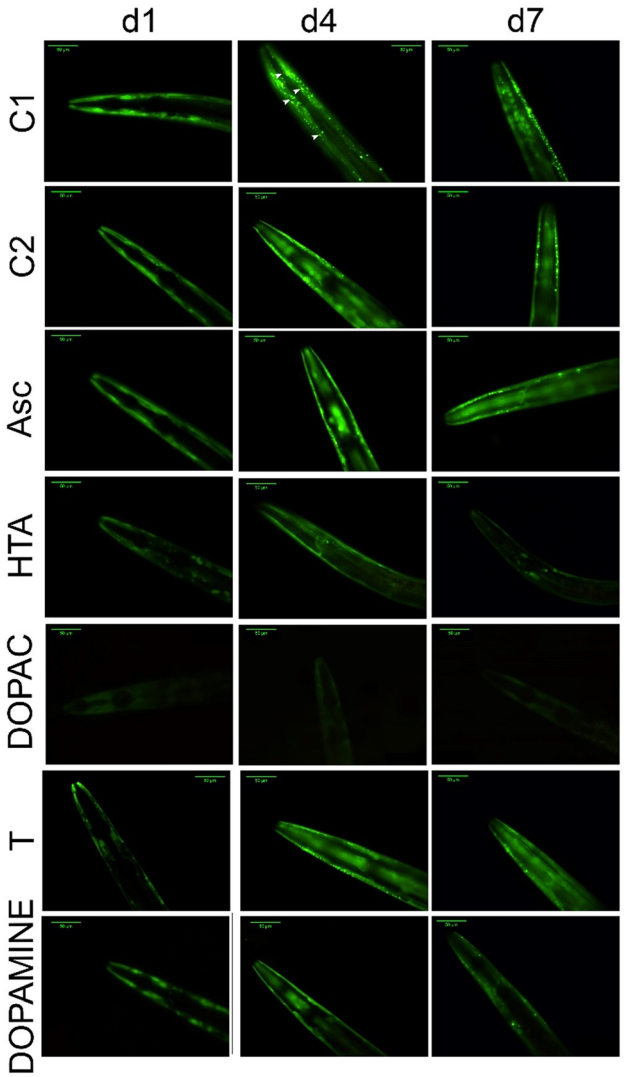

Fig. 5 Effects of different phytochemicals on the *C. elegans* Parkinson's disease model. Representative images of the NL5901 strain with or without treatments over time. d1, d4, and d7 correspond to the first, fourth, and seventh days of the nematode's adulthood, respectively. The arrowheads indicate αS aggregates formed in the animal muscle cells. C1 is the control condition and C2 shows representative images of *C. elegans* treated with 1 mM sodium ascorbate. The biomolecules sodium ascorbate (Asc), hydroxytyrosol acetate (HTA), DOPAC, tyrosol (T) and dopamine were supplemented at 15 mM and stabilized with sodium ascorbate at 1 mM. Scale bar: 50 μm.

mechanisms. Hydroxytyrosol acetate is a metabolite of dopamine that has been shown to possess antioxidant properties.[12] It can scavenge reactive oxygen species and prevent oxidative stress, which is known to promote the aggregation of αS. Additionally, hydroxytyrosol acetate can modulate the activity of enzymes involved in αS aggregation, such as tyrosinase and monoamine oxidase, thereby reducing the formation of toxic aggregates. Meanwhile, DOPAC is a major metabolite of dopamine produced by the action of the enzyme monoamine oxidase.[39] DOPAC has been found to inhibit αS aggregation by direct interaction with αS and so, it disrupts the fibrillation

 This journal is © The Royal Society of Chemistry 2024

Open Access Article. Published on 16 May 2024. Downloaded on 1/29/2025 4:27:49 PM.
This article is licensed under a Creative Commons Attribution-NonCommercial 3.0 Unported Licence.

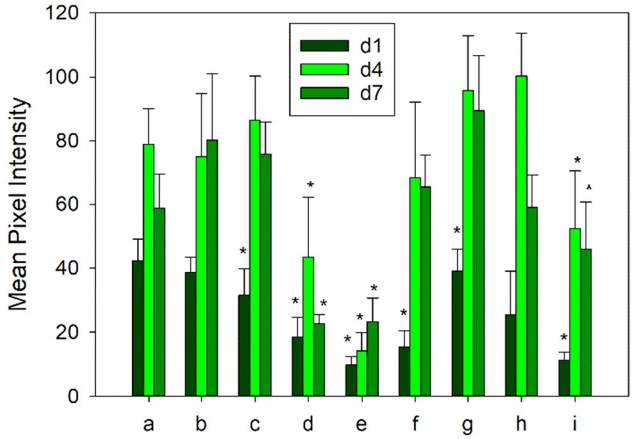

Fig. 6 Bioactive molecule effect on αS aggregation *in vivo*. The graph shows the quantification of αS expression *in vivo* under different conditions. (a) Control. (b) Control with 1 mM sodium ascorbate. (c) Sodium ascorbate at 15 mM. (d) Hydroxytyrosol acetate, 15 mM, stabilized with sodium ascorbate. (e) DOPAC, 15 mM, stabilized with sodium ascorbate. (f) Hydroxytyrosol, 15 mM, stabilized with sodium ascorbate. (g) Tyrosol, 15 mM, stabilized with sodium ascorbate. (h) L-Dopa at 1.14 mM stabilized with sodium ascorbate. (i) Dopamine, 15 mM, stabilized with sodium ascorbate. Data are shown as mean ± standard deviation, * significant at p-value ≤ 0.05 by ANOVA test using Bonferroni *post hoc* test. Two independent experiments were performed, and a minimum of 20 individuals were analyzed.

process, thus preventing the formation of toxic aggregates.[40] Furthermore, hydroxytyrosol acetate can modulate the expression of proteins able to hinder αS aggregation. Also, hydroxytyrosol acetate has been shown to increase the expression of heat shock proteins, which are known to have chaperone activity and can assist in the appropriate folding of proteins. This can prevent the misfolding and aggregation of αS.[41] Overall, the inhibitory effects of hydroxytyrosol acetate and DOPAC on αS aggregation may involve, in addition to the direct interaction with the protein demonstrated in the bimolecular fluorescence cellular model, a combination of antioxidant properties, modulation of related enzyme activities, and regulation of the cellular mechanisms of protein folding and degradation.

Bioactive molecule effect on *C. elegans* lifespan

Lifespan is defined as the time elapsed from the birth of an organism until its death. It is a parameter widely used in studies of aging and diseases associated with aging, such as Alzheimer's, Huntington's, or Parkinson's. Parkinson's disease model nematodes were treated with different bioactive molecules to analyze a possible effect on their longevity. Hydroxytyrosol acetate (15 mM) significantly increased the mean and maximum lifespan by 28.5 and 14.4%, respectively, in comparison with those of the control animals treated with ascorbate (Fig. S3A and B, Table S4†). Similarly, DOPAC (15 mM), sodium ascorbate (15 mM), and dopamine (15 mM) also exerted a positive effect on the longevity of *C. elegans*, increasing the mean lifespan by 25.6, 20.2, and 14.1%, respectively (Fig. S3A–C, and Table S4†). In addition, DOPAC increased the maximum lifespan by 20.0%. The effect of tyrosol, hydroxytyrosol, and L-dopa on lifespan was not significant; however, as stated before, their effect on αS aggregation was lost with time. Sodium ascorbate at high concentration (15 mM) showed a moderate effect on the oligomerization of αS in nematodes, yet it prolonged the mean lifespan of the animals. These results indicate that lifespan is affected by additional factors in addition to the formation of αS aggregates, such as the production of reactive oxygen species and the subsequent increase of oxidative stress in nematodes. Other studies have shown that certain polyphenols, such as baicalein, prolonged the lifespan of wild-type animals (strain N2) by reducing oxidative stress *in vivo* and modulating genes able to activate the animal's detoxification pathways.[42]

Conclusions

The αS-BiFC cell model was used to estimate the efficacy of four polyphenols present in olive oil (tyrosol, hydroxytyrosol, hydroxytyrosol acetate, and DOPAC), two polyphenols present in plants as secondary metabolites (L-dopa and dopamine), and vitamin C as αS antiaggregating agents. The most active molecules were hydroxytyrosol acetate (HTA) with an EC_{50} value of 1.97 mM and sodium ascorbate with an EC_{50} value of 2.81 mM. In addition, at concentrations up to 15 mM, both HTA and DOPAC decreased the cell fluorescence and thus the rate of αS oligomerization by 100%. PAMPA showed that HTA presents the highest permeation capacity through brain lipids among the substances used in this study, including the prescribed drug for Parkinson's disease, L-dopa.

The Parkinson's disease model of *Caenorhabditis elegans* used allowed the evaluation of the effects of the selected molecules *in vivo*. The compounds that decreased αS aggregation the most *in vivo* were HTA (76.2%) and DOPAC (79.2%). Moreover, dopamine also reduced the aggregates by 67.4% in the *in vivo* assay. Additionally, the compounds HTA and DOPAC also exhibited a positive effect on the longevity of *C. elegans*, increasing the average lifespan by 28.5% and 25.6%, respectively.

As hypothesized, naturally occurring tyrosols were able to reduce αS aggregation *in vitro* and *in vivo*. Furthermore, due to their structure, the compounds performed better than L-dopa and dopamine in the PAMPA permeability assay. Thus, the results of this work open a new avenue to the use of olive oil dietary molecules as nutraceuticals to treat Parkinson's disease, with HTA and DOPAC being the polyphenols with the most promising results.

Author contributions

S. H.-G., B. G.-C., P. H.-E., P. M.-R., and F. G.-H. conceived the research. S. H.-G., B. G.-C., P. H.-E., and P. M.-R. designed, performed and interpreted all the experiments under the supervi-

Open Access Article. Published on 16 May 2024. Downloaded on 1/29/2025 4:27:49 PM. This article is licensed under a Creative Commons Attribution-NonCommercial 3.0 Unported Licence.

sion of F. G.-H. S. H.-G. and B. G.-C. wrote the manuscript, which was contributed by all authors. F. G.-H. obtained the funds. All authors read and approved the manuscript.

Ethical statement

Ethical approval for this study was obtained from the CEEA (Ethics Committee for Animal Experimentation) of the home institution "University of Murcia" with the report number 778/2022.

Conflicts of interest

The authors declare that they have no known competing financial interests or personal relationships that could influence the work reported in this paper.

Acknowledgements

This work was supported by the Spanish Ministry of Science and Innovation project PID2021-122896NB-I00 (MCI/AEI/10.13039/501100011033/FEDER, UE). P. M.-R. thanks the Fundación Séneca for the contract 21587/FPI/21.

References

1 L. C. Shukla, J. Schulze, J. Farlow, N. D. Pankratz, J. Wojcieszek and T. Foroud, *Gene Reviews*, 2019.
2 M. A. Menéndez and L. F. Morgenstern, *Rev. Española Discapac.*, 2013, **1**, 25–49.
3 R. García-Ramos, E. L. Valdés, L. Ballesteros, S. Jesús and P. Mir, *Neurologia*, 2016, **31**, 401–413.
4 B. R. Bloem, M. S. Okun and C. Klein, *Lancet*, 2021, **397**, 2284–2303.
5 J. Benito-León, *Rev. Neurol.*, 2018, **66**, 125–134.
6 R. Di Maio, E. K. Hoffman, E. M. Rocha, M. T. Keeney, L. H. Sanders, B. R. De Miranda, A. Zharikov, A. Van Laar, A. F. Stepan, T. A. Lanz, J. K. Kofler, E. A. Burton, D. R. Alessi, T. G. Hastings and J. Timothy Greenamyre, *Sci. Transl. Med.*, 2018, **10**, 451.
7 N. B. Mercuri and G. Bernardi, *Trends Pharmacol. Sci.*, 2005, **26**, 341–344.
8 P. Huot, T. H. Johnston, J. B. Koprich, S. H. Fox and J. M. Brotchie, *Pharmacol. Rev.*, 2013, **65**, 171–222.
9 A. Tresserra-Rimbau and R. M. Lamuela-Raventós, *Olives olive oil as Funct. foods Bioactivity, Chem. Process*, 2017, pp. 417–434.
10 J. Rodríguez-Morató, L. Xicota, M. Fitó, M. Farré, M. Dierssen and R. De La Torre, *Molecules*, 2015, **20**, 4655–4680.
11 C. Salis, L. Papageorgiou, E. Papakonstantinou, M. Hagidimitriou and D. Vlachakis, *GeNeDis 2018 Genet. Neurodegener*, 2020, pp. 77–91.
12 A. Karković Marković, J. Torić, M. Barbarić and C. Jakobušić Brala, *Molecules*, 2019, **24**, 2001.
13 J. G. Fernandez-Bolanos, O. Lopez, J. Fernandez-Bolanos and G. Rodriguez-Gutierrez, *Curr. Org. Chem.*, 2008, **12**, 442–463.
14 D. Storga, K. Vrecko, J. G. D. Birkmayer and G. Reibnegger, *Neurosci. Lett.*, 1996, **203**, 29–32.
15 K. C. Hughes, X. Gao, I. Y. Kim, E. B. Rimm, M. Wang, M. G. Weisskopf, M. A. Schwarzschild and A. Ascherio, *Mov. Disord.*, 2016, **31**, 1909–1914.
16 H. Nagayama, M. Hamamoto, M. Ueda, C. Nito, H. Yamaguchi and Y. Katayama, *Clin. Neuropharmacol.*, 2004, **27**, 270–273.
17 F. Calahorro and M. Ruiz-Rubio, *Invertebr. Neurosci.*, 2011, **11**, 73–83.
18 S. Saha, M. D. Guillily, A. Ferree, J. Lanceta, D. Chan, J. Ghosh, C. H. Hsu, L. Segal, K. Raghavan and K. Matsumoto, *J. Neurosci.*, 2009, **29**, 9210–9218.
19 M. Markaki and N. Tavernarakis, *Curr. Opin. Biotechnol.*, 2020, **63**, 118–125.
20 T. Long, Q. Wu, J. Wei, Y. Tang, Y.-N. He, C.-L. He, X. Chen, L. Yu, C.-L. Yu, B. Y.-K. Law, J.-M. Wu, D.-L. Qin, A.-G. Wu and X.-G. Zhou, *Oxid. Med. Cell. Longevity*, 2022, **2022**, 3723567, DOI: **10.1155/2022/3723567**.
21 T. A. Eastwood, K. Baker, H. R. Brooker, S. Frank and D. P. Mulvihill, *FEBS Lett.*, 2017, **591**, 833–841.
22 C. A. Schneider, W. S. Rasband and K. W. Eliceiri, *Nat. Methods*, 2012, **9**, 671–675.
23 E. Studzińska-Sroka, A. Majchrzak-Celińska, P. Zalewski, D. Szwajgier, E. Baranowska-Wójcik, M. Żarowski, T. Plech and J. Cielecka-Piontek, *Cancers*, 2021, **13**, 1717.
24 T. Stiernagle, *WormBook*, 2006, pp. 1–11.
25 P. Alvarez-Illera, P. García-Casas, J. Arias-del-Val, R. I. Fonteriz, J. Alvarez and M. Montero, *Oncotarget*, 2017, **8**, 55889–55900.
26 M. A. Guerrero-Rubio, S. Hernández-García, F. García-Carmona and F. Gandía-Herrero, *Food Chem.*, 2019, **274**, 840–847.
27 A. Zafra-Gómez, B. Luzón-Toro, S. Capel-Cuevas and J. C. Morales, *Food Nutr. Sci.*, 2011, **2**(10), 1114–1120, DOI: **10.4236/fns.2011.210149**.
28 M. Gallardo-Fernández, M. Gonzalez-Ramirez, A. B. Cerezo, A. M. Troncoso and M. C. Garcia-Parrilla, *Foods*, 2022, **11**, 2355.
29 N. and A. (NDA) EFSA Panel on Dietetic Products,D. Turck, J. Bresson, B. Burlingame, T. Dean, S. Fairweather–Tait, M. Heinonen, K. I. Hirsch–Ernst, I. Mangelsdorf and H. J. McArdle, *EFSA J.*, 2017, **15**, e04728.
30 M. Robles-Almazan, M. Pulido-Moran, J. Moreno-Fernandez, C. Ramirez-Tortosa, C. Rodriguez-Garcia, J. L. Quiles and Mc. Ramirez-Tortosa, *Food Res. Int.*, 2018, **105**, 654–667.
31 J. M. Pérez de la Lastra, C. M. Curieses Andrés, C. Andrés Juan, F. J. Plou and E. Pérez-Lebeña, *Foods*, 2023, **12**, 1937.

 This journal is © The Royal Society of Chemistry 2024

Open Access Article. Published on 16 May 2024. Downloaded on 1/29/2025 4:27:49 PM.
This article is licensed under a Creative Commons Attribution-NonCommercial 3.0 Unported Licence.

32 M. Masuda, N. Suzuki, S. Taniguchi, T. Oikawa, T. Nonaka, T. Iwatsubo, S. I. Hisanaga, M. Goedert and M. Hasegawa, *Biochemistry*, 2006, **45**, 6085–6094.
33 S. Di Giovanni, S. Eleuteri, K. E. Paleologou, G. Yin, M. Zweckstetter, P. A. Carrupt and H. A. Lashuel, *J. Biol. Chem.*, 2010, **285**, 14941–14954.
34 J. Pujols, S. Peña-Díaz, D. F. Lázaro, F. Peccati, F. Pinheiro, D. González, A. Carija, S. Navarro, M. Conde-Giménez and J. García, *Proc. Natl. Acad. Sci. U. S. A.*, 2018, **115**, 10481–10486.
35 Y. A. Wang, L. van Sluijs, Y. Nie, M. G. Sterken, S. C. Harvey and J. E. Kammenga, *Genes*, 2020, **11**, 1–10.
36 G. Oikonomou and S. Shaham, *Glia*, 2011, **59**, 1253–1263.
37 N. Saewanee, T. Praputpittaya, N. Malaiwong, P. Chalorak and K. Meemon, *Neurosci. Res.*, 2021, **162**, 13–21.
38 S. Hughes, M. van Dop, N. Kolsters, D. van de Klashorst, A. Pogosova and A. M. Rijs, *Pharmaceuticals*, 2022, **15**, 512.
39 C. Chen and Y. Wei, *J. Funct. Foods*, 2021, **82**, 104506.
40 L. Palazzi, B. Fongaro, M. Leri, L. Acquasaliente, M. Stefani, M. Bucciantini and P. Polverino de Laureto, *Int. J. Mol. Sci.*, 2021, **22**, 6008.
41 J. M. Romero-Márquez, M. D. Navarro-Hortal, V. Jiménez-Trigo, P. Muñoz-Ollero, T. Y. Forbes-Hernández, A. Esteban-Muñoz, F. Giampieri, I. Delgado Noya, P. Bullón and L. Vera-Ramírez, *Antioxidants*, 2022, **11**, 629.
42 M. A. Guerrero-Rubio, S. Hernández-García, F. García-Carmona and F. Gandía-Herrero, *Antioxidants*, 2021, **10**, 438.